Original Article

Comparison of aortic blood flow rotational direction in healthy volunteers and patients with bicuspid aortic valves using volumetric velocity-sensitive cardiovascular magnetic resonance imaging

Sebastian Ebel[1,2]^, Benjamin Köhler[3], Abhinav Aggarwal[4], Bernhard Preim[3], Benjamin Behrendt[3], Bernd Jung[5], Robin F. Gohmann[1], Boris Riekena[1], Michael Borger[6], Philipp Lurz[7], Timm Denecke[2], Matthias Grothoff[1#], Matthias Gutberlet[1#]

[1]Department of Diagnostic and Interventional Radiology, University of Leipzig – Heart Centre, Leipzig, Germany; [2]Department of Diagnostic and Interventional Radiology, University of Leipzig, Leipzig, Germany; [3]Department of Simulation and Graphics, University of Magdeburg, Magdeburg, Germany; [4]Department of Radiology, Saral Diagnostics, New Delhi, India; [5]Department of Diagnostic, Interventional and Paediatric Radiology, University of Bern, Bern, Switzerland; [6]Department of Cardiac Surgery, University Leipzig – Heart Centre, Leipzig, Germany; [7]Department of Cardiology, University Leipzig – Heart Centre, Leipzig, Germany

Contributions: (I) Conception and design: S Ebel, M Borger, P Lurz, T Denecke, M Grothoff, M Gutberlet; (II) Administrative support: B Preim, T Denecke, M Grothoff, M Gutberlet; (III) Provision of study materials or patients: S Ebel, B Köhler, B Preim, B Behrendt, M Borger, P Lurz, M Grothoff, M Gutberlet; (IV) Collection and assembly of data: S Ebel, A Aggarwal, RF Gohmann, B Riekena; (V) Data analysis and interpretation: S Ebel, B Köhler, B Preim, B Behrendt, B Jung, RF Gohmann, B Riekena, M Gutberlet; (VI) Manuscript writing: All authors; (VII) Final approval of manuscript: All authors.

[#]These authors contributed equally to this work.

Correspondence to: Sebastian Ebel, MD. Department of Diagnostic and Interventional Radiology, University of Leipzig – Heart Centre, Leipzig, Germany; Department of Diagnostic and Interventional Radiology, University of Leipzig, Liebigstrasse 20, 04103 Leipzig, Germany. Email: sebastian.ebel@icloud.com.

Background: The rotational direction (RD) of helical blood flow can be classified as either a clockwise (RD^+) or counter-clockwise (RD^-) flow. We hypothesized that this simple classification might not be sufficient for analysis *in vivo* and a simultaneous existence of $RD^{+/-}$ may occur. We utilized volumetric velocity-sensitive cardiovascular magnetic resonance imaging (4D flow MRI) to analyze rotational blood flow in the thoracic aorta.

Methods: Forty volunteers (22 females; mean age, 41±16 years) and seventeen patients with bicuspid aortic valves (BAVs) (9 females; mean age, 42±14 years) were prospectively included. The RDs and the calculation of the rotating blood volumes (RBVs) in the thoracic aorta were performed using a pathline-projection strategy.

Results: We could confirm a mainly clockwise RD in the ascending, descending aorta and in the aortic arch. Furthermore, we found a simultaneous existence of RD^+/RD^-. The $RD^{+/-}$-volume in the ascending aorta was significantly higher in BAV patients, the mean RD^+/RD^- percentage was approximately 80%/20% *vs.* 60%/40% in volunteers (P<0.01). The maximum RBV always occurred during systole. There was significantly more clockwise than counter-clockwise rotational flow in the ascending aorta (P<0.01) and the aortic arch (P<0.01), but no significant differences in the descending aorta (P=0.48).

^ ORCID: 0000-0001-6856-6455.

© Quantitative Imaging in Medicine and Surgery. All rights reserved.

Conclusions: A simultaneous occurrence of RD^+/RD^- indicates that a simple categorization in either of both is insufficient to describe blood flow *in vivo*. Rotational flow in the ascending aorta and in the aortic arch differs significantly from flow in the descending aorta. BAV patients show significantly more clockwise rotating volume in the ascending aorta compared to healthy volunteers.

Keywords: Volumetric velocity-sensitive cardiovascular magnetic resonance imaging (4D flow MRI); helical blood flow; rotational direction (RD); aortic blood flow; bicuspid aortic valve (BAV); rotating blood volume (RBV)

Submitted Feb 14, 2023. Accepted for publication Sep 13, 2023. Published online Oct 27, 2023.
doi: 10.21037/qims-23-183
View this article at: https://dx.doi.org/10.21037/qims-23-183

Introduction

The evaluation of fluid dynamics in human vessels is a fast-expanding topic (1,2). With the emerge of time-resolved, three-directional, three-dimensional (3D) phase-contrast cardiac magnetic resonance imaging (MRI) [termed volumetric velocity-sensitive cardiovascular (4D flow) MRI], there is growing interest regarding hemodynamic phenomena, especially in the thoracic aorta (3-7). Recent studies have shown that flow phenomena like helical flow contribute to the distribution and intensity of wall shear stress (WSS), which is an important parameter in terms of understanding the development of aortic dilatation or type B dissection chirality (8-10). It has been shown, that in the setting of bicuspid aortic valve (BAV) and subsequent aortic dilatation, there are markedly elevated secondary flow parameters. One of these parameters for assessing helical flow is the rotational direction (RD) of flow, which was mostly classified as either a clockwise or counter-clockwise rotation (11,12). However, it could be demonstrated that in a curved pipe, like the human aorta, flow does not either show clockwise or counter-clockwise rotation, but more likely both RDs simultaneously. This behaviour of fluids was stated to be normal and could additionally already be proven in an experimental setting of closed curved pipes, completely filled with liquids (13). This suggests that a simple distinction between a clockwise or counter-clockwise flow rotations and description of its proportional distribution might be insufficient for a definite differentiation between physiological and pathophysiologic blood flow in the thoracic aorta.

4D flow enables the non-invasive assessment and visualization of cardiovascular blood flow. Besides absolute flow quantification, 4D flow allows the visualization and measurement of different flow parameters like helical flow or the analysis of the RD of flow (14). These new parameters might be useful for the surveillance of patients with aortic pathologies, help to adapt patient management, and finally identify the right moment for therapeutic interventions.

Furthermore, the identification of the main RD of helical blood flow might be needed, as well as absolute quantification. However, the clinical value of these new qualitative and quantitative flow parameters is still not clear, and therefore, they are not yet included in the clinical routine and decision-making process.

Thus, the aim of this study was to utilize 4D flow in order to elucidate the rotational flow direction and for the first time to absolutely quantify the rotational blood volume within the ascending aorta, in the aortic arch and in the thoracic descending aorta in healthy volunteers and in patients with different types of BAVs.

Methods

Study cohort

Forty healthy volunteers with no history of cardiovascular disease (CVD) (22 females; mean age, 41±16 years) and seventeen patients with BAV (9 females; mean age, 42±14 years) were included in this study. We characterized the different types of BAV as suggested by Sievers *et al.* (15), a commonly used classification in the clinical routine. The BAV morphology was assessed by MRI. The blood pressure was measured at the beginning of the MRI scan. The stage of aortic regurgitation and stenosis was determined by MRI and classified according to the American College of Cardiology (ACC)/American Heart Association (AHA) guidelines, where stage A means no regurgitation volume and no flow acceleration >2 m/s (16). Additionally, we characterized the types of the aortic arch as suggested by Zhang *et al.* (17): the aortic arch can be

© Quantitative Imaging in Medicine and Surgery. All rights reserved.

divided into three types according to the ratio between the diameter of the common carotid artery to the distance between the horizontal line through the top of the arch and the horizontal line through the orifice of innominate artery. Patients with other abnormalities or impaired left ventricular function were excluded. The study was conducted in accordance with the Declaration of Helsinki (as revised in 2013). The study was approved by the institutional ethics committee of the University of Leipzig (No. AZ 443/16-ek) and informed consent was taken from all the patients.

Magnetic resonance image acquisition

The 4D flow datasets were acquired at a 3-T scanner using a 16-channel anterior surface coil in combination with a 12-element-spine coil (Magnetom Verio Dot, Siemens Healthcare GmbH, Erlangen, Germany). Imaging parameters were: repetition time (TR) =3.2 ms, echo time (TE) =2.8 ms, flip angle 10°, acquisition matrix 320 mm × 240 mm with a mean temporal resolution of 39.2 ms and a spatial resolution of 2.5×2.5×2.5 mm^3, velocity encoding (VENC) 150 cm/s, phase encoding direction anterior to posterior, slice number 24. The used sequence was evaluated before (18,19).

Cardiac magnetic resonance data analysis

Vessel segmentation, blood flow visualization, and pre-processing

We corrected for phase wraps, eddy currents and background noise as described previously (20,21). All processing and measurement steps were carried out using the custom-made software tool "Bloodline" (22). The segmentation of the aorta and the placement of the centreline was performed automatically as described by Köhler *et al.* (22). The ascending aorta was defined as the volume of the aorta between the aortic valve and the origin of the brachiocephalic trunk, the aortic arch was defined as the volume between the origin of the brachiocephalic trunk and the left subclavian artery, and the thoracic descending aorta was defined as the volume between the origin of the left subclavian artery and the diaphragm. Bloodline enables the analysis of defined regions of interest, e.g., the ascending aorta, the aortic arch or the thoracic descending aorta and provides the volume of the segmented vessel (in mL). Aortic blood flow was visualized using time-resolved pathlines.

Measurements and flow quantifications

All measurements were carried out by one observer with more than 7 years of experience in cardiac MRI (Ebel S). The aortic volume and diameter were given out automatically by the software Bloodline and were defined as the volume in ml and the largest diameter perpendicular to the vessels' centreline of the section of interest (e.g., ascending aorta, aortic arch, or descending aorta). The RD of helical flow was subdivided into clockwise (right-handed, viewed in downstream direction—RD^+) or counter-clockwise (left-handed—RD^-) flow. RD was assessed as described by Meuschke *et al.* (23) and Köhler *et al.* (24): for each point of the centre line of the aorta the software bloodline calculates a virtual xy-plane perpendicular to the vessels course (the centre line). The orientation of the first virtual plane (on the first point of the centerline) is determined using the cross product of the plane's normal vector (i.e., the centerline) and global x-, y-, and z-axis of the MRI dataset. All subsequent planes are iteratively oriented based on the preceding plane and the rotation between it and the preceding planes normal vector, ensuring a consistent orientation between all planes. Each plane can be subdivided into four quadrants (Q1–Q4) (*Figure 1*). The RD was determined for each pathline segment that consisted of two successive points. The spacing between each point was approximately 1 mm and the temporal distance between singular pathline points is 5–7.5 ms. Both points are projected in the xy-plane of the first point. For these projected points, we identified the angle to the x-axis of the plane. This angle's size indicates in which quadrant of the plane the points are located. For example, suppose the successive points are located in the first and second quadrants (Q1 and Q2). In that case they present an RD^+ segment (*Figure 1A*). If the points are located in the third and fourth quadrants (Q3 and Q4), a left-handed or RD^- segment exists (*Figure 1B*). If they are located in diagonal quadrants, the intersection between the connecting line and the y-axis is used to define a RD (*Figure 1C*). Depending on whether a pathline has more right or left rotating segments, it is classified as RD^+ or RD^-. Therefore, the RD depends on the amount of RD^+ or RD^- pathlines. Two points in Q1 could be "missed" despite exhibiting a counter-clockwise rotation of 80 degrees. However, under the assumption that the flow is not highly chaotic, that the following pathline segment would display a similar counter-clockwise rotation, which would put the next point firmly into quadrant

© Quantitative Imaging in Medicine and Surgery. All rights reserved.

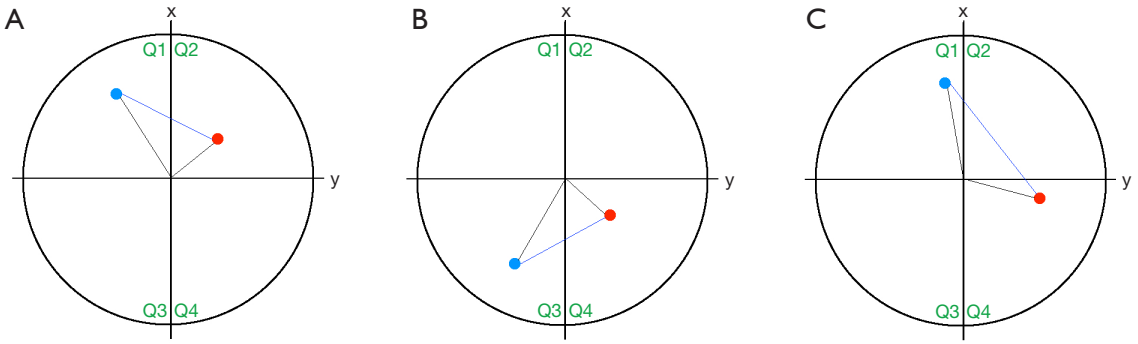

Figure 1 Three examples for the determination of the rotation direction in the cross-sectional plane. The lines from the blue point (first) to the red point (second) are pathline segments that are projected into a plane. (A) The successive points are in the first and second quadrant (Q1 and Q2), they represent a right-handed segment. (B) The successive points are in the fourth and third (Q4 and Q3) quadrant, they represent a left-handed segment. (C) The points are in diagonal quadrants (Q1 and Q4), in this case they represent a right-handed segment.

Q3, causing the segment to be recognized as a counter-clockwise rotation. With this technique, pathlines with two consecutive points located within the same quadrant (e.g., Q1 and Q1) are not considered as rotating flow and are therefore ignored. Pathlines were generated as described elsewhere (22). This method extracts all kinds of rotating blood flow, not only helical or vortical flow. A helix is defined as a flow phenomenon of a rotational, corkscrew-like pattern with an antegrade forward motion, whereas vortical flow is defined as a flow pattern with a revolving flow volume on the spot around a common axis without any forward motion. However, the differentiation between helical and vortical flow might be difficult because there is a smooth transition between both phenomena and definite cut-offs do not exist.

The absolute and relative volume in mL or % of clockwise and counter-clockwise rotating blood in different sections of the thoracic aorta was assessed as follows.

The averaged rotating blood volume (RBVav)

The clockwise or counter-clockwise RBV averaged over one cardiac cycle calculated as an absolute value in mL. Additionally, since this internally corrects for absolute volume of the vessel, we calculated the relative RBV in % based on the total flow volume in ascending aorta, the aortic arch or the descending aorta, respectively.

The RBV—occurrence

The temporal occurrence of peak RBV within the cardiac cycle was measured in ms and as a relative value in % based on the length of the cardiac cycle.

Additionally, the RD's spatial distribution was assessed in a qualitatively using heatmaps of the aorta.

Statistical analysis

All analyses were performed using SPSS (SPSS Statistics V27, IBM, Armonk, NY, USA). Quantitative variables were expressed as mean values and standard deviations (SDs). For patients and volunteers, data were tested for normal distribution using the Shapiro-Wilk test. Once a Gaussian distribution was confirmed, paired correlations analysis comparing clockwise and counter-clockwise rotational volumes (RV) in patients and volunteers were performed using an independent sample *t*-test. For comparison of the different aortic arch types, Wilcoxon-Mann-Whitney test was performed. Additionally, Pearson correlation analysis to determine the relationship between RBV and aortic size has been performed. For P value adjustment after multiple *t*-test Bonferroni correction was performed. A P value <0.05 was considered statistically significant.

Results

Volunteer and patient characteristics

We included six subjects with BAV Sievers-type left coronary-right coronary (L-R), five subjects with type left coronary-non-coronary (L-N), and six subjects with type right coronary-non-coronary (R-N). BAV patients had no significant impairment of the aortic valve [no stage > A for aortic stenosis/regurgitation according to the ACC/AHA guidelines (16)] (P=0.21). Types of the aortic arch according

© Quantitative Imaging in Medicine and Surgery. All rights reserved.

Table 1 Volunteer and patient characteristics

Characteristics	Volunteers	BAV patients			
		Type L-R	Type L-N	Type R-N	All types
N [female]	40 [22]	6 [4]	5 [4]	6 [1]	17 [9]
Age (years)	41±16	39±16	44±11	43±15	42±14
Resting heart rate (beats/min)	70±12	69±10	61±9	59±5	63±9
Blood pressure (mmHg)	117/82±7/6	128/76±9/3	119/81±7/4	122/65±6/6	123/74±7/9
Cardiac output (L/min)	4.2±2.9	4.4±3.1	4.5±1.8	4.3±1.0	4.4±1.7
BMI (kg/m^2)	24.3±5.1	26.2±3.5	24.3±6.2	24.8±1.1	25.1±3.8
BSA (m^2)	1.89±0.3	1.89±0.5	1.88±0.7	1.81±0.7	1.86

Data are presented as N [n], mean ± SD, or mean. BAV, bicuspid aortic valve; L-R, left coronary-right coronary; L-N, left coronary-non-coronary; R-N, right coronary-non-coronary; BMI, body mass index; BSA, body surface area; SD, standard deviation.

to Zhang *et al.*: type I, (29 volunteers and 12 patients); type II (11 volunteers and 4 patients), III (0 volunteers and 1 patient) (17). All participants had a left-sided aortic arch and descending thoracic aorta.

The mean resting heart rate and blood pressure during the examination was 70±12 beats/min and 117/82±7/6 mmHg in volunteers and 63±9 beats/min and 123/74±7/9 mmHg in patients. The mean cardiac output was 4.2±2.9 L/min in volunteers and 4.4±1.7 L/min in patients. The mean body mass index (BMI) was 24.3±5.1 kg/m^2 in volunteers and 25.1±3.8 kg/m^2 in patients, without significance, respectively (P=0.14, 0.20, 0.15). The mean body surface area (BSA) of volunteers and patients were 1.89 m^2 and 1.86 m^2, respectively without significant differences (P=0.51). The mean volumes of the ascending aorta, the aortic arch, and the descending aorta in volunteers were 35.1±11.5, 17.4±5.8, and 34.1±11.4 mL and 84.1±17.9, 33.1±11.8, and 37.2±13.7 mL in patients, respectively. With significant larger values in patients in the ascending aorta and the aortic arch (P<0.001, respectively), while there were no significant differences regarding the descending aorta (P=0.67). The ascending aorta diameter in patients ranged from 34 to 45 mm (n=6 with an ascending aorta diameter of <40 mm: n=1 with Sievers type L-R, n=2 with type L-N, n=3 with type R-N). The mean diameters of the ascending aorta and aortic arch were significant larger in patients as compared to volunteers (P<0.001) with 39±16 *vs.* 28±9 mm, while there were no significant differences in the aortic arch (27±8 *vs.* 33±9 mm) and the descending aorta (28±9 *vs.* 29±6 mm) (P=0.54 and P=0.67). Volunteer and patient characteristics are given in *Tables 1*,*2*.

RBVav

In volunteers, the mean RBV_{av} in the ascending aorta was 10.7±4.3 mL. And 6.4±1.2 mL rotated in clockwise direction (RBV_{av}^{+}) while (RBV_{av}^{-}) was 4.3±1.3 mL. That means that 31.2% of the blood volume in the ascending aorta of volunteers was rotating. There was no relevant correlation between size of the ascending aorta (r=0.23, P>0.05), aortic arch (r=0.28, P>0.05), and descending aorta (r=0.21, P>0.05), and RBV_{av} in volunteers (see *Table 2*).

In BAV patients, the mean RBV_{av} was 36.3±4.2 mL, meaning that 43.6% of the blood volume of the ascending aorta was rotating, which is significantly more than in healthy individuals (P<0.01, respectively). This was also true for patients with an ascending aorta diameter of <40 mm. Interestingly, the RBV_{av} in BAV patients with a normal-sized ascending aorta (<40 mm) is significant higher compared to volunteers (40.6%±9.1% *vs.* 31.2%±7.6%, P>0.05). The RD in the ascending aorta was also mostly clockwise and the mean RBV_{av}^{+} was significantly higher as compared to volunteers with 28.2±3.3 mL and the RBV_{av}^{-} significantly less (P<0.01) with 8.1±3.1 mL. There was a moderate and significant correlation between size of the ascending aorta (r=0.73, P<0.05) and aortic arch (r=0.61, P<0.05) and RBV_{av} in patients, but not for the size of the descending aorta (r=0.25, P>0.05) and RBV_{av}.

In patients with BAV Sievers type L-R, the mean RBV_{av}^{+} in the ascending aorta was 25.1±4.6 mL and the mean RBV_{av}^{-} was 8.3±1.9 mL. In patients with BAV Sievers type L-N, the RBV_{av}^{+} in the ascending aorta was 16.2±3.9 mL and the RBV_{av}^{-} was 11.1±1.6 mL. In patients with BAV Sievers type R-N, the RBV_{av}^{+} in the ascending aorta was

© Quantitative Imaging in Medicine and Surgery. All rights reserved.

Table 2 RBVs in volunteers and patients

Parameters	Measurement ± SD	Maximum ascending aorta diameter ± SD (mm)	Correlation coefficient r/P value
Volunteers		289	
Mean averaged rotating volume (mL)	10.7±4.3		0.23/0.53
Percentage of RBV (%)	31.2±7.6		0.28/0.47
Patients overall with ascending aorta diameter <40 mm		345	
Mean averaged rotating volume (mL)	26.9±3.4		0.54/<0.05
Percentage of RBV (%)	40.6±9.1		0.58/<0.05
Patients overall		3,916	
Mean averaged rotating volume (mL)	36.3±4.2		0.73/<0.05
Percentage of RBV (%)	43.6±17.1		0.77/<0.05
Patients subtype Sievers L-R		4,218	
Mean averaged rotating volume (mL)	33.4±3.7		0.69/<0.05
Percentage of RBV (%)	40.8±19.0		0.74/<0.05
Patients subtype Sievers L-N		3,611	
Mean averaged rotating volume (mL)	27.3±1.7		0.72/<0.05
Percentage of RBV (%)	39.1±23.6		0.77/<0.05
Patients subtype Sievers R-N		428	
Mean averaged rotating volume (mL)	58.8±5.6		0.78/<0.05
Percentage of RBV (%)	56.6±21.7		0.81/<0.05

SD, standard deviation; RBV, rotating blood volume; L-R, left coronary-right coronary; L-N, left coronary-non-coronary; R-N, right coronary-non-coronary.

49.1±6.3 mL and RBV_{av}^{-} was 9.7±3.3 mL. All patient subgroups showed significantly higher RBV_{av}^{+} and RBV_{av}^{-} compared to volunteers and in subtype R-N we found significant higher RBV_{av}^{+} and RBV_{av}^{-} as compared to patients overall and the other subtypes (P<0.001, respectively). There were no significant differences between the different morphologic aortic arch types.

The results indicate that there is generally more clockwise than counter-clockwise rotating flow in the ascending aorta in volunteers (P<0.01), which further increases in BAV patients as well as the absolute rotating volumes (P<0.01). Similar results could be achieved in the aortic arch (P<0.01, respectively) but not in the thoracic descending aorta. Detailed results are given in *Tables 2,3*.

Analysis of the spatial distribution of RBVav

A specific spatial flow distribution occurred in the aortic arch of all volunteers; counter-clockwise flow aligned at the outer surface of the vessel, right at the origins of the supra-aortic vessels, while clockwise flow aligned at the inner surface of the aortic arch. No specific spatial distribution patterns of clockwise and counter-clockwise flow could be detected in the ascending and descending aorta (*Figure 2*). This was true for all morphologic aortic arch types.

In BAV patients, there was no such alignment of clock- and counter-clockwise flow in the aortic arch. The spatial distribution in all parts of the thoracic aorta seemed to be arbitrary. There were no differences regarding the spatial distribution of clock- and counter-clockwise flow between the different BAV subgroups. The spatial distribution of clockwise and counter-clockwise flow averaged over one cardiac cycle in a volunteer and a BAV patient are shown in *Figure 2*.

Temporal occurrence of RBV within the cardiac cycle

In healthy volunteers clockwise peak rotational blood volume (RBV^{+}) in the ascending aorta occurred on average

© Quantitative Imaging in Medicine and Surgery. All rights reserved.

Table 3 Clockwise and counter-clockwise RBVs in volunteers and patients

Parameters	Ascending aorta		Aortic arch		Thoracic descending aorta	
	Mean ± SD	P value†	Mean ± SD	P value†	Mean ± SD	P value†
Volunteers		<0.01		<0.01		0.48
Mean averaged clockwise rotating volume (mL)	6.4±1.2		4.2±0.7		3.1±0.2	
Mean averaged clockwise rotating volume (%)	59.8±11.2		59.2±9.8		68.9±4.4	
Mean averaged counter-clockwise rotating volume (mL)	4.3±1.3		2.9±0.8		1.4±0.3	
Mean averaged counter-clockwise rotating volume (%)	40.2±12.1		40.8±11.3		31.1±6.7	
Patients overall		<0.01/<0.01		<0.01/<0.01		0.31/0.24
Mean averaged clockwise rotating volume (mL)	28.2±3.3		17.6±2.7		5.8±2.1	
Mean averaged clockwise rotating volume (%)	77.7±9.1		65.7±10.1		57.4±20.8	
Mean averaged counter-clockwise rotating volume (mL)	8.1±3.1		9.2±2.1		4.3±1.7	
Mean averaged counter-clockwise rotating volume (%)	22.3±8.5		34.3±7.8		42.6±16.8	
Patients subtype Sievers 1 L-R (n=6)		<0.01/<0.01/0.64		<0.01/<0.01/0.36		0.60/0.73/0.23
Mean averaged clockwise rotating volume (mL)	25.1±4.6		13.1±3.3		5.3±3.0	
Mean averaged clockwise rotating volume (%)	75.1±13.7		61.8±15.6		54.6±30.9	
Mean averaged counter-clockwise rotating volume (mL)	8.3±1.9		8.1±1.7		4.4±1.9	
Mean averaged counter-clockwise rotating volume (%)	24.9±5.6		38.2±8.0		43.4±19.6	
Patients subtype Sievers 1 L-N (n=5)		<0.01/<0.01/0.21		<0.01/<0.01/0.10		0.41/0.51/0.57
Mean averaged clockwise rotating volume (mL)	16.2±3.9		12.9±2.2		4.8±2.1	
Mean averaged clockwise rotating volume (%)	59.3±14.3		61.4±10.5		53.9±23.6	
Mean averaged counter-clockwise rotating volume (mL)	11.1±1.6		8.1±1.9		4.1±1.1	
Mean averaged counter-clockwise rotating volume (%)	40.7±5.9		38.6±9		46.1±12.4	
Patients subtype Sievers 1 R-N (n=6)		<0.01/<0.01/<0.01		<0.01/<0.01/<0.01		0.11/0.28/0.46
Mean averaged clockwise rotating volume (mL)	49.1±6.3		44.7±7.9		6.1±1.9	
Mean averaged clockwise rotating volume (%)	83.5±11.5		87.8±15.5		54.0±16.8	
Mean averaged counter-clockwise rotating volume (mL)	9.7±3.3		6.2±3.0		5.2±2.6	
Mean averaged counter-clockwise rotating volume (%)	16.5±16.4		12.2±5.9		46.0±23.0	

Distribution of the measurements of the mean average clockwise and counter-clockwise RV averaged over one cardiac cycle and peak RV in millilitres and % (based on the flow volumes in the corresponding vessel section) in the ascending aorta, the aortic arch, and the thoracic descending aorta. Comparisons between percentages of clockwise and counterclockwise flow volumes. †, comparison between clockwise and counter-clockwise/patients and volunteers/patients and patients overall. RBV, rotating blood volume; SD, standard deviation; L-R, left coronary-right coronary; L-N, left coronary-non-coronary; R-N, right coronary-non-coronary; RV, rotational volume.

© Quantitative Imaging in Medicine and Surgery. All rights reserved.

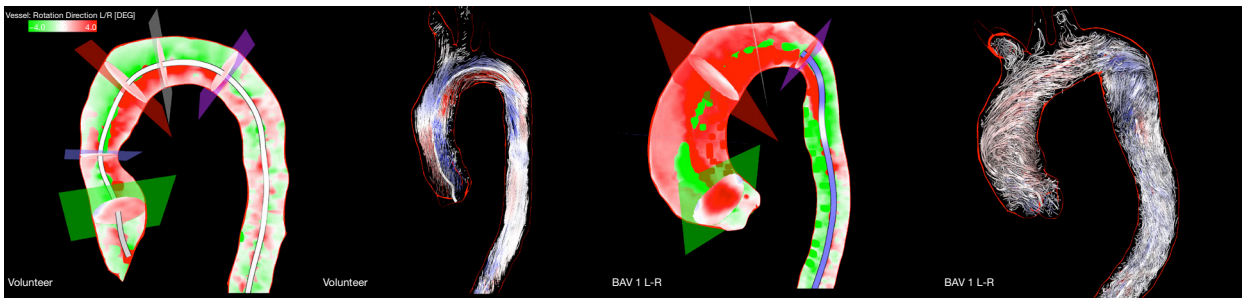

Figure 2 Visualization of a RD map on the surface of the thoracic aorta and as pathlines. Please note that in the volunteer the aortic arch counter-clockwise flow aligns at the outer surface of the vessel, while clockwise flow aligns at the inner surface of the aorta, while there is no such alignment in the patient. In the ascending and descending aorta clockwise and counter-clockwise flow are not separated. In the volunteer the pathlines on the outer surface of the aortic arch seems to go predominantly into the supraaortic vessels. Volunteer: 29 years old female. Patient: 27 years old female, BAV type L-R. BAV, bicuspid aortic valve; L-R, left coronary-right coronary; RD, rotational direction.

at 245.57±18.18 ms/27.07%±2.00% of the cardiac cycle. Counter-clockwise peak rotational blood volume (RBV^-) in the ascending aorta occurred almost simultaneously with RBV^+ on average at 236.20±22.53 ms/26.41%±2.48%, with no significant differences between RBV^+ and RBV^- (see *Table 4*). In the ascending aorta of patients (overall), RBV^+ occurred on average at 241.33±17.92 ms/24.28%±1.80% of the cardiac cycle, RBV^- occurred on average at 233.17±19.21 ms/23.46%±1.93% of the cardiac cycle. There were neither significant differences between volunteers and patients (overall), nor between the different BAV subgroups (see *Table 4*). In summary, in all subjects RBV^+ and RBV^- occurred almost simultaneously during systole.

Discussion

4D flow enables the visualization of rotational flow and subsequently its categorization as either clockwise or counter-clockwise (11,12). With the introduced technique for extraction and analysis of rotating flow, we were able to quantify the exact volume of clockwise and counter-clockwise rotating blood semi-automatically and were able to differentiate quantitatively rotating and non-rotating flow. We found significantly higher RBVs in the ascending aorta and the aortic arch in BAV patients compared to healthy volunteers, which is in line with other studies, that found elevated rotating flow in BAV patients (25). There are other techniques for extracting only helical and vortical flow, like the λ_2 criterion or a pressure-based approach (26,27). The latter technique has been described and used for analysis of healthy volunteers and BAV patients and it has been stated that helices in BAV patients are larger and last longer compared to healthy volunteers (27). The proposed method for rotational flow analysis in this current study, considers all kinds of rotating flow: laminar, turbulent, helical, and vortical. The authors believe that not only one kind of flow or only one parameter can be held responsible for the occurrence of complications in BAV patients like the development of aortic aneurysms or dissection, but flow abnormalities "in toto". We, therefore, assume that the proposed method to absolutely quantify RBV might give a more comprehensive picture of complex flow conditions *in vivo*.

Contrarily to an "either/or-classification", we could demonstrate both—clockwise and counter-clockwise rotation—existing in healthy volunteers and in BAV patients. These results aligned with experimental observations in closed, curved pipes completely filled with fluid in which clockwise and counter-clockwise flow also coincided whenever the fluid was pushed downstream (28). From a simplistic point of view, the aorta can also be seen as a closed pipe, whereas the ascending and the descending aorta are the straight and the aortic arch the curved part. However, we could also detect more clockwise than counter-clockwise RBVs in all parts of the thoracic aorta, which is in line with the 4D flow literature, in which right-handed (clockwise) flow has been described as a non-pathologic and the dominant flow feature in humans (29,30).

Furthermore, we demonstrated that in BAV patients, clockwise rotating blood flow was significantly elevated compared to healthy volunteers: The ratio between rotating and non-rotating flow in the ascending aorta in volunteers was about 30/70 while it was about 45/55 in BAV patients. These findings are consistent with other sources which

© Quantitative Imaging in Medicine and Surgery. All rights reserved.

Table 4 Occurrence of RBVs in volunteers and patients

Parameters	Ascending aorta		Aortic arch		Thoracic descending aorta	
	Mean ± SD	P value†	Mean ± SD	P value†	Mean ± SD	P value†
Volunteers		0.78		0.66		0.41
Occurrence of clockwise peak RBV (ms)	245.57±18.18		277.64±13.66		291.80±17.86	
Occurrence of clockwise peak RBV (%)	27.07±2.00		30.61±1.51		32.17±1.97	
Occurrence of counter-clockwise peak RBV (ms)	236.20±22.53		293.53±19.43		316.05±29.01	
Occurrence of counter-clockwise peak RBV (%)	26.41±2.48		32.36±2.14		34.85±3.20	
Patients overall		0.29/0.23		0.74/0.64		0.47/0.62
Occurrence of clockwise peak RBV (ms)	241.33±17.92		278.84±14.19		299.78±19.44	
Occurrence of clockwise peak RBV (%)	24.28±1.80		28.05±1.43		30.16±1.96	
Occurrence of counter-clockwise peak RBV (ms)	233.17±19.21		289.50±17.33		311.34±18.18	
Occurrence of counter-clockwise peak RBV (%)	23.46±1.93		26.97±1.74		31.32±1.83	
Patients subtype Sievers 1 L-R (n=6)		0.21/0.25		0.33/0.47		0.19/0.13
Occurrence of clockwise peak RBV (ms)	242.55±15.18		277.33±21.88		294.92±18.79	
Occurrence of clockwise peak RBV (%)	23.83±1.49		27.69±2.13		28.97±1.85	
Occurrence of counter-clockwise peak RBV (ms)	235.92±9.20		268.09±19.06		305.77±24.40	
Occurrence of counter-clockwise peak RBV (%)	23.17±0.90		26.33±1.87		30.04±2.40	
Patients subtype Sievers 1 R-N (n=6)		0.14/0.23		0.18/0.25		0.41/0.32
Occurrence of clockwise peak RBV (ms)	249.41±19.17		281.91±21.70		297.48±18.99	
Occurrence of clockwise peak RBV (%)	26.96±2.07		30.48±2.35		32.16±2.05	
Occurrence of counter-clockwise peak RBV (ms)	234.33±29.11		271.22±31.09		297.44±28.28	
Occurrence of counter-clockwise peak RBV (%)	25.33±3.15		29.32±3.36		32.16±3.06	
Patients subtype Sievers 1 L-N (n=5)		0.21/0.18		0.41/0.31		0.71/0.80
Occurrence of clockwise peak RBV (ms)	243.33±11.91		278.40±16.38		298.53±11.09	
Occurrence of clockwise peak RBV (%)	22.78±1.12		26.07±1.53		27.95±1.04	
Occurrence of counter-clockwise peak RBV (ms)	238.73±17.11		271.90±16.41		300.04±21.29	
Occurrence of counter-clockwise peak RBV (%)	22.35±1.60		25.46±1.54		28.10±1.99	

Distribution of the measurements of the mean peak clockwise and counter-clockwise RV in mL and % (based on the flow volumes in the corresponding vessel section) and the time of the occurrence of peak RBV in ms and % (based on the length of the cardiac cycle) in the ascending aorta, the aortic arch and the thoracic descending aorta. Comparisons between percentages of clockwise and counterclockwise flow volumes. †, comparison between clockwise and counter-clockwise/patients and volunteers. RBV, rotating blood volume; SD, standard deviation; L-R, left coronary-right coronary; L-N, left coronary-non-coronary; R-N, right coronary-non-coronary; RV, rotational volume.

© Quantitative Imaging in Medicine and Surgery. All rights reserved.

described an increased helicity or helical fraction index in BAV patients compared to healthy individuals (31,32). These results indicate that the absolute quantification of these newly introduced parameters might be suitable for further differentiation between physiological and pathological flow. Additionally, we found elevated RBV also in patients with a rather normal ascending aorta diameter of <40 mm, but RBV was greatest in patients with dilated ascending aorta, meaning that both factors, the dilatation of the aorta and the bicuspidity of the aortic valve are important factors. Based on these findings, one can hypothesize, that the flow alterations are causing dilatation, which might worsen the flow alterations which leads to more dilatation in a "downward spiral manner".

The mean relative $RBV_{av}^{+}/RBV_{av}^{-}$ ratio in the ascending aorta indicating the percentage of clockwise *vs.* counter-clockwise flow was approximately 60%/40% in healthy volunteers and approximately 80%/20% in BAV patients. To the best of our knowledge, this is the first study describing this.

In 2012, Bürk *et al.* analyzed the rotational strength in healthy volunteers and patients with dilated ascending aorta (11). They subdivided rotational flow in small (<180°), moderate (180–360°), or "supra-physiological" flow (>360°) like suggested by Bieging *et al.* (33). Visual analysis by two experienced observers performed this grading. In this study, they found increased strength in patients compared to controls, fitting with our results. However, the described rotational strength analysis was based on visual observations of the rotational movement. This might work for clearly visible rotational flow but is not quantitative and might therefore suffer from inter-observer-variability. To overcome this issue other groups conducted techniques which include artificial intelligence (AI) and found that fully automated analysis of complex aortic flow dynamics like rotational flow from 4D flow is feasible using AI (34).

Additionally to the findings of previous 4D flow studies (29,30), we assume that both, right- and left-handed rotational blood flow can be pathological flow features. Therefore, we hypothesize that not the rotational flow direction itself, but the absolute or relative volume of rotating blood could be helpful to differentiate between physiological and pathological flow patterns. Those results partially fit with the literature: Bissell *et al.* analysed 3D flow phenomena in subjects with BAV and found "abnormal right-handed helical flow in the ascending aorta" compared to healthy volunteers (35). They concluded that flow abnormalities in BAV patients might be a major contributor to aortic dilatation. Similar results were conducted by Dux-Santoy *et al.* describing increased rotational flow in BAV patients (36).

Contrary, to our findings at the ascending aorta and the aortic arch, we found no significant differences between patients and volunteers in the descending aorta. Therefore, it seems that the alteration of the rotating blood flow in the setting of BAV mainly affects the ascending aorta and the aortic arch. This could be an explanation, why aortic dilatation in BAV patients mainly occurs in the ascending aorta and the aortic arch, because it is known that there is a strong link between elevated rotational flow and elevated WSS and aortic root and arch dilatation (37-40). In our analysis, the Pearson correlation to investigate the relationship between RBV and the diameter of the ascending aorta demonstrated an overall good correlation between the absolute and relative RBV and the maximal aortic diameter of the ascending aorta in patients from 0.69–0.81. Bollache *et al.* found that in BAV patients, increased WSS is significantly associated with elastic fibre thinning in the ascending aorta leading to aortic dilation (41). The authors assume that the parameter WSS measures the entirety of factors or forces, which act on the vessel wall: e.g., flow parameters like RBV, the shape of the aorta or blood pressure.

Further analysis revealed that in patients and in volunteers the maximum rotating blood flow occurred independently from its flow direction always during systole, which is in line with the findings of Kilner *et al.* (30), who found so-called "spiral" flow also predominantly during systole.

We could detect significant differences of the RBV between the ascending aorta and the descending aorta and between the aortic arch and the descending aorta in patients and in volunteers. Possible reasons for these observations could either be the higher peak velocities in the ascending aorta and the aortic arch due to the spatial proximity to the heart, and the curved shape of the left ventricular outflow tract, the ascending aorta and the aortic arch, while the descending aorta has a straight course. The latter explanation would be in line with the literature. Dean *et al.*, e.g., demonstrated that there are more secondary flow patterns, like rotational flow in a curved pipe than in straight tubes (42,43). Another fact, that would underline the hypothesis that the loss of rotational flow in the descending aorta is due to the straight course of the vessel is, that in patients with abdominal aortic aneurysms there are elevated secondary flow patterns within the aneurysm

© Quantitative Imaging in Medicine and Surgery. All rights reserved.

and closely distally to it (44). In other words, it seems that there is non-rotational flow in straight vessels while there is rotational flow in curved vessels.

Therefore, it emerges, that rotational blood flow was more pronounced and maybe more important in the ascending aorta and the aortic arch than in the thoracic descending aorta. One could hypothesize that the described rotational flow patterns are important for the filling of the coronary arteries and the supra-aortic branches: it has been shown that unique flow phenomena like vortical flow seem to be important for the filling of the coronary vessels, and in *Figure 2* there seems to be a predominant flow of the outer pathlines into the supraaortic vessels, but there is no clear evidence for this hypothesis (29). Additionally, the group around Frydrychowicz *et al.* described vortices at the orifices of the supra-aortic branches in healthy individuals and patients after aortic coarctation repair (45). In our study, we also found that in volunteers counter-clockwise rotating flow seems to align at the outer surface of the aortic arch, right at the origins of the supra-aortic vessels. Interestingly, we found no such alignment of rotating flow in the aortic arch of BAV patients. Therefore, the alteration of RBV_{av} in the ascending aorta seems to affect the distribution of rotating flow downstream. There was no significance of the different aortic arch types. Therefore, the authors hypothesize, that not the aortic arch type influences the flow patterns in the aortic arch but more the flow patterns and distributions in the ascending aorta.

One major limitation of this study is the rather small sample size of patients (n=17). This might be the reason for a largely even distribution of the three BAV subtypes, which differs from the prevalence in the literature. However, despite the small sample size a significant larger mean RBV_{av} in the BAV Sievers R-N subtype compared to the other two could be demonstrated (*Table 2*). Additionally, we could only include one subject with an aortic arch type III, and therefore it was not possible to perform reliable statistical analysis. However, this first study was thought to be a proof of principle. Additionally, we only assessed the volume of rotating blood but not the rotational strength. As described in the methods section the technique used in this study considers only rotating pathline segments of rotational flow that exceeds a certain threshold. E.g., Garcia *et al.* conducted a study that analysed 65 healthy subjects and 50 BAV patients and found elevated rotational strength using a quantitative approach (25). For future studies, combining both methods to analyse the RBVs and the rotational strength could be beneficial. Additionally, there are no repeatability data, but since we used an automated, software-based approach for aortic segmentation, there should be no relevant inter-reader variance. In addition, the assessment of the RD's spatial distribution was only performed qualitatively. This is because the used software tool is not capable of doing so, yet. To the best of our knowledge no commercially available tool allows for detailed, quantitative analysis of the spatial distribution of the RD within, e.g., the aortic arch. This should be addressed in future studies.

Conclusions

We could demonstrate that clockwise and counter-clockwise rotational flow occurs simultaneously in healthy volunteers and BAV patients. Furthermore, we showed that rotational flow in the ascending aorta and the aortic arch differs significantly from rotational flow in the thoracic descending aorta. Additionally, we demonstrated that the newly introduced quantitative parameter RBV_{av} in the ascending aorta is significantly higher in BAV patients compared to healthy individuals and is positively correlated with the maximal aortic diameter in BAV patients. The physiological meaning of these observations has to be evaluated in further studies.

We state that not the rotational flow direction itself but the volume of rotating blood and the distribution of RD^+/RD^- might help in the assessment of aortic pathologies.

Acknowledgments

Funding: The study was supported by a DFG-grant (GU 777/4-1 AOBJ 629068 and GR 4617/2-1 AOBJ 629069).

Footnote

Conflicts of Interest: All authors have completed the ICMJE uniform disclosure form (available at https://qims.amegroups.com/article/view/10.21037/qims-23-183/coif). AA was supported by an ESOR/ESCR 2019 cardiac fellowship. The other authors have no conflicts of interest to declare.

Ethical Statement: The authors are accountable for all aspects of the work in ensuring that questions related to the accuracy or integrity of any part of the work are appropriately investigated and resolved. The study was conducted in accordance with the Declaration of Helsinki (as revised in 2013). The study was approved by the institutional ethics committee of the University of Leipzig

© Quantitative Imaging in Medicine and Surgery. All rights reserved.

(No. AZ 443/16-ek) and informed consent was taken from all the patients.

Open Access Statement: This is an Open Access article distributed in accordance with the Creative Commons Attribution-NonCommercial-NoDerivs 4.0 International License (CC BY-NC-ND 4.0), which permits the non-commercial replication and distribution of the article with the strict proviso that no changes or edits are made and the original work is properly cited (including links to both the formal publication through the relevant DOI and the license). See: https://creativecommons.org/licenses/by-nc-nd/4.0/.

References

1. Grotberg JB, Jensen OE. Biofluid mechanics in flexible tubes. Annu Rev Fluid Mech 2004;36:121-7.
2. Liepsch D. Biofluid mechanics. Biomed Tech (Berl) 1998;43:94-9.
3. Ku DN, Giddens DP, Zarins CK, Glagov S. Pulsatile flow and atherosclerosis in the human carotid bifurcation. Positive correlation between plaque location and low oscillating shear stress. Arteriosclerosis 1985;5:293-302.
4. Malek AM, Alper SL, Izumo S. Hemodynamic shear stress and its role in atherosclerosis. JAMA 1999;282:2035-42.
5. Cunningham KS, Gotlieb AI. The role of shear stress in the pathogenesis of atherosclerosis. Lab Invest 2005;85:9-23.
6. Shaaban AM, Duerinckx AJ. Wall shear stress and early atherosclerosis: a review. AJR Am J Roentgenol 2000;174:1657-65.
7. Stam K, Chelu RG, van der Velde N, van Duin R, Wielopolski P, Nieman K, Merkus D, Hirsch A. Validation of 4D flow CMR against simultaneous invasive hemodynamic measurements: a swine study. Int J Cardiovasc Imaging 2019;35:1111-8.
8. Salerno M, Chandrashekhar Y. CMR 4D-Flow Wall Shear Stress and Aortic Dilation in Bicuspid Aortic Valve. JACC Cardiovasc Imaging 2022;15:177-9.
9. Zhang J, Rothenberger SM, Brindise MC, Markl M, Rayz VL, Vlachos PP. Wall Shear Stress Estimation for 4D Flow MRI Using Navier-Stokes Equation Correction. Ann Biomed Eng 2022;50:1810-25.
10. Bondesson J, Suh GY, Lundh T, Dake MD, Lee JT, Cheng CP. Quantification of true lumen helical morphology and chirality in type B aortic dissections. Am J Physiol Heart Circ Physiol 2021;320:H901-11.
11. Bürk J, Blanke P, Stankovic Z, Barker A, Russe M, Geiger J, Frydrychowicz A, Langer M, Markl M. Evaluation of 3D blood flow patterns and wall shear stress in the normal and dilated thoracic aorta using flow-sensitive 4D CMR. J Cardiovasc Magn Reson 2012;14:84.
12. Lorenz R, Bock J, Barker AJ, von Knobelsdorff-Brenkenhoff F, Wallis W, Korvink JG, Bissell MM, Schulz-Menger J, Markl M. 4D flow magnetic resonance imaging in bicuspid aortic valve disease demonstrates altered distribution of aortic blood flow helicity. Magn Reson Med 2014;71:1542-53.
13. Remke K. Pedley, T. J., The Fluid Mechanics of Large Blood Vessels. Cambridge Monographs on Mechanics and Applied Mathematics. Cambridge-New York-Melbourne, Cambridge University Press 1980. XV, 446 S., ISBN 0-521-22626-0. Journal of Applied Mathematics and Mechanics 1981;61:207.
14. van der Geest RJ, Garg P. Advanced Analysis Techniques for Intra-cardiac Flow Evaluation from 4D Flow MRI. Curr Radiol Rep 2016;4:38.
15. Sievers HH, Schmidtke C. A classification system for the bicuspid aortic valve from 304 surgical specimens. J Thorac Cardiovasc Surg 2007;133:1226-33.
16. Otto CM, Nishimura RA, Bonow RO, Carabello BA, Erwin JP 3rd, Gentile F, Jneid H, Krieger EV, Mack M, McLeod C, O'Gara PT, Rigolin VH, Sundt TM 3rd, Thompson A, Toly C. 2020 ACC/AHA Guideline for the Management of Patients With Valvular Heart Disease: A Report of the American College of Cardiology/American Heart Association Joint Committee on Clinical Practice Guidelines. Circulation 2021;143:e72-e227.
17. Zhang Q, Ma X, Zhang W, Wang Z, Zhang H, Zhang X, Song J, Zou C. Surgical repair and reconstruction of aortic arch in debakey type I aortic dissection: recent advances and single-center experience in the application of branched stent graft. J Cardiothorac Surg 2017;12:86.
18. Ebel S, Hübner L, Köhler B, Kropf S, Preim B, Jung B, Grothoff M, Gutberlet M. Validation of two accelerated 4D flow MRI sequences at 3 T: a phantom study. Eur Radiol Exp 2019;3:10.
19. Ebel S, Dufke J, Köhler B, Preim B, Rosemeier S, Jung B, Dähnert I, Lurz P, Borger M, Grothoff M, Gutberlet M. Comparison of two accelerated 4D-flow sequences for aortic flow quantification. Sci Rep 2019;9:8643.
20. Bock J, Kreher BW, Hennig J, Markl M. Optimized pre-processing of time-resolved 2D and 3D phase contrast MRI data. In: Proceedings of the 15th Annual meeting of ISMRM. Berlin; 2007;15:3138.
21. Dyverfeldt P, Bissell M, Barker AJ, Bolger AF, Carlhäll

© Quantitative Imaging in Medicine and Surgery. All rights reserved.

CJ, Ebbers T, Francios CJ, Frydrychowicz A, Geiger J, Giese D, Hope MD, Kilner PJ, Kozerke S, Myerson S, Neubauer S, Wieben O, Markl M. 4D flow cardiovascular magnetic resonance consensus statement. J Cardiovasc Magn Reson 2015;17:72.
22. Köhler B, Grothoff M, Gutberlet M, Preim B. Bloodline: A system for the guided analysis of cardiac 4D PC-MRI data. Computers & Graphics 2019;82:32-43.
23. Meuschke M, Köhler B, Preim U, Preim B, Lawonn K. Semi-automatic vortex flow classification in 4D PC-MRI data of the aorta. Computer Graphics Forum 2016;35:351-60.
24. Köhler B, Preim U, Grothoff M, Gutberlet M, Fischbach K, Preim B. Robust cardiac function assessment in 4D PC-MRI data of the aorta and pulmonary artery. Comput Graph Forum 2016;35:32-43.
25. Garcia J, Barker AJ, Collins JD, Carr JC, Markl M. Volumetric quantification of absolute local normalized helicity in patients with bicuspid aortic valve and aortic dilatation. Magn Reson Med 2017;78:689-701.
26. Schafhitzel T, Vollrath JE, Gois JP, Weiskopf D, Castelo A, Ertl T. Topology-Preserving λ2-based Vortex Core Line Detection for Flow Visualization. Comput Graph Forum 2008;27:1023-30.
27. Ebel S, Dufke J, Köhler B, Preim B, Behrendt B, Riekena B, Jung B, Stehning C, Kropf S, Grothoff M, Gutberlet M. Automated Quantitative Extraction and Analysis of 4D flow Patterns in the Ascending Aorta: An intraindividual comparison at 1.5 T and 3 T. Sci Rep 2020;10:2949.
28. Ku DN. Blood flow in arteries. Annu Rev Fluid Mech 1997;29:399-434.
29. Markl M, Draney MT, Hope MD, Levin JM, Chan FP, Alley MT, Pelc NJ, Herfkens RJ. Time-resolved 3-dimensional velocity mapping in the thoracic aorta: visualization of 3-directional blood flow patterns in healthy volunteers and patients. J Comput Assist Tomogr 2004;28:459-68.
30. Kilner PJ, Yang GZ, Mohiaddin RH, Firmin DN, Longmore DB. Helical and retrograde secondary flow patterns in the aortic arch studied by three-directional magnetic resonance velocity mapping. Circulation 1993;88:2235-47.
31. Cao K, Atkins SK, McNally A, Liu J, Sucosky P. Simulations of morphotype-dependent hemodynamics in non-dilated bicuspid aortic valve aortas. J Biomech 2017;50:63-70.
32. Youssefi P, Gomez A, He T, Anderson L, Bunce N, Sharma R, Figueroa CA, Jahangiri M. Patient-specific computational fluid dynamics-assessment of aortic hemodynamics in a spectrum of aortic valve pathologies. J Thorac Cardiovasc Surg 2017;153:8-20.e3.
33. Bieging ET, Frydrychowicz A, Wentland A, Landgraf BR, Johnson KM, Wieben O, François CJ. In vivo three-dimensional MR wall shear stress estimation in ascending aortic dilatation. J Magn Reson Imaging 2011;33:589-97.
34. Garrido-Oliver J, Aviles J, Córdova MM, Dux-Santoy L, Ruiz-Muñoz A, Teixido-Tura G, Maso Talou GD, Morales Ferez X, Jiménez G, Evangelista A, Ferreira-González I, Rodriguez-Palomares J, Camara O, Guala A. Machine learning for the automatic assessment of aortic rotational flow and wall shear stress from 4D flow cardiac magnetic resonance imaging. Eur Radiol 2022;32:7117-27.
35. Bissell MM, Hess AT, Biasiolli L, Glaze SJ, Loudon M, Pitcher A, Davis A, Prendergast B, Markl M, Barker AJ, Neubauer S, Myerson SG. Aortic dilation in bicuspid aortic valve disease: flow pattern is a major contributor and differs with valve fusion type. Circ Cardiovasc Imaging 2013;6:499-507.
36. Dux-Santoy L, Guala A, Teixidó-Turà G, Ruiz-Muñoz A, Maldonado G, Villalva N, Galian L, Valente F, Gutiérrez L, González-Alujas T, Sao-Avilés A, Johnson KM, Wieben O, Huguet M, García-Dorado D, Evangelista A, Rodríguez-Palomares JF. Increased rotational flow in the proximal aortic arch is associated with its dilation in bicuspid aortic valve disease. Eur Heart J Cardiovasc Imaging 2019;20:1407-17.
37. Ebel S, Kühn A, Aggarwal A, Köhler B, Behrendt B, Gohmann R, Riekena B, Lücke C, Ziegert J, Vogtmann C, Preim B, Kropf S, Jung B, Denecke T, Grothoff M, Gutberlet M. Quantitative normal values of helical flow, flow jets and wall shear stress of healthy volunteers in the ascending aorta. Eur Radiol 2022;32:8597-607.
38. Hope MD, Hope TA, Crook SE, Ordovas KG, Urbania TH, Alley MT, Higgins CB. 4D flow CMR in assessment of valve-related ascending aortic disease. JACC Cardiovasc Imaging 2011;4:781-7.
39. den Reijer PM, Sallee D 3rd, van der Velden P, Zaaijer ER, Parks WJ, Ramamurthy S, Robbie TQ, Donati G, Lamphier C, Beekman RP, Brummer ME. Hemodynamic predictors of aortic dilatation in bicuspid aortic valve by velocity-encoded cardiovascular magnetic resonance. J Cardiovasc Magn Reson 2010;12:4.
40. Beroukhim RS, Kruzick TL, Taylor AL, Gao D, Yetman AT. Progression of aortic dilation in children with a functionally normal bicuspid aortic valve. Am J Cardiol 2006;98:828-30.

© Quantitative Imaging in Medicine and Surgery. All rights reserved.

41. Bollache E, Guzzardi DG, Sattari S, Olsen KE, Di Martino ES, Malaisrie SC, van Ooij P, Collins J, Carr J, McCarthy PM, Markl M, Barker AJ, Fedak PWM. Aortic valve-mediated wall shear stress is heterogeneous and predicts regional aortic elastic fiber thinning in bicuspid aortic valve-associated aortopathy. J Thorac Cardiovasc Surg 2018;156:2112-2120.e2.
42. Dean WR. XVI. Note on the motion of fluid in a curved pipe. The London, Edinburgh, and Dublin Philosophical Magazine and Journal of Science 1927;4:208-23.
43. Dean WR. LXXII. The stream-line motion of fluid in a curved pipe (Second paper). The London, Edinburgh, and Dublin Philosophical Magazine and Journal of Science 1928;5:673-95.
44. Takehara Y. Clinical Application of 4D Flow MR Imaging for the Abdominal Aorta. Magn Reson Med Sci 2022;21:354-64.
45. Frydrychowicz A, Markl M, Hirtler D, Harloff A, Schlensak C, Geiger J, Stiller B, Arnold R. Aortic hemodynamics in patients with and without repair of aortic coarctation: in vivo analysis by 4D flow-sensitive magnetic resonance imaging. Invest Radiol 2011;46:317-25.

Cite this article as: Ebel S, Köhler B, Aggarwal A, Preim B, Behrendt B, Jung B, Gohmann RF, Riekena B, Borger M, Lurz P, Denecke T, Grothoff M, Gutberlet M. Comparison of aortic blood flow rotational direction in healthy volunteers and patients with bicuspid aortic valves using volumetric velocity-sensitive cardiovascular magnetic resonance imaging. Quant Imaging Med Surg 2023;13(12):7973-7986. doi: 10.21037/qims-23-183

© Quantitative Imaging in Medicine and Surgery. All rights reserved.